Journal of Biomolecular NMR, 7 (1996) 99–106
ESCOM

J-Bio NMR 333

Three-dimensional ^{1}H-TOCSY-relayed ct-[^{13}C,^{1}H]-HMQC for aromatic spin system identification in uniformly ^{13}C-labeled proteins

Oliver Zerbe*, Thomas Szyperski, Marcel Ottiger and Kurt Wüthrich**

Institut für Molekularbiologie und Biophysik, Eidgenössische Technische Hochschule-Hönggerberg, CH-8093 Zürich, Switzerland

Received 21 December 1995
Accepted 10 January 1996

Keywords: Resonance assignments; Aromatic spin systems; ^{13}C-labeled proteins; HMQC

Summary

Three-dimensional ^{1}H-TOCSY-relayed ct-[^{13}C,^{1}H]-HMQC is a novel experiment for aromatic spin system identification in uniformly ^{13}C-labeled proteins, which is implemented so that it correlates the chemical shift of a given aromatic proton with those of the directly attached carbon and all vicinal protons. The ct-HMQC scheme is used both for overlay of the indirect ^{1}H and ^{13}C chemical shift evolution periods and for the generation of ^{1}H-^{1}H antiphase magnetization to accelerate the ^{1}H-TOCSY magnetization transfer at short mixing times. As an illustration, data recorded for the 18 kDa protein cyclophilin A are presented. Since transverse relaxation of ^{13}C-^{1}H zero-quantum and double-quantum coherences is to first order insensitive to ^{13}C-^{1}H heteronuclear dipolar relaxation, the new experiment should work also for proteins with molecular weights above 20 kDa.

Introduction

Aromatic amino acids play a pivotal role in the architecture of the hydrophobic core in proteins. Hence, complete assignment of the aromatic spin systems is a key factor for obtaining high-quality NMR structures of proteins. Sequence-specific assignments of aromatic residues are usually achieved in two steps. One is the identification of the aromatic spin systems via scalar connectivities. Two-dimensional (2D) [^{1}H,^{1}H]-TOCSY and [^{1}H,^{1}H]-COSY have traditionally been employed for unlabeled proteins (Wüthrich, 1986), while 2D ω_2(^{13}C)-half-filtered [^{1}H,^{1}H]-TOCSY (Otting and Wüthrich, 1990; Szyperski et al., 1994), 2D constant-time (ct) HCCH-TOCSY (e.g., Damberger et al., 1994; Logan et al., 1994) or 2D ^{1}H-TOCSY-relayed ct-[^{13}C,^{1}H]-HSQC experiments (Archer et al., 1993) have been used for uniformly ^{13}C-labeled proteins. In the other step, sequence-specific assignments are obtained via NOEs observed between the aromatic ^{1}H spin systems and the β-methylene protons (Wüthrich, 1986), either in 2D [^{1}H,^{1}H]-NOESY for unlabeled proteins (Wüthrich, 1986), or in 3D ^{13}C-resolved [^{1}H,^{1}H]-NOESY (Ikura et al., 1990) and/or 2D ω_2(^{13}C)-half-filtered [^{1}H,^{1}H]-NOESY (Otting and Wüthrich, 1990; Szyperski et al., 1994) for ^{13}C-labeled proteins. Two experiments have also been proposed that use scalar couplings to establish connectivities between the aromatic spin systems and ^{13}C$^{\beta}$ in ^{13}C-labeled proteins (Yamazaki et al., 1993; Grzesiek and Bax, 1995a). However, in spite of this impressive repertoire of NMR experiments, the assignment of aromatic spin systems remains a challenging task for larger proteins because of the typically very limited ^{1}H and ^{13}C chemical shift dispersion and the presence of large one-bond ^{13}C-^{13}C scalar couplings. Recently, 'reverse labeling' has been proposed for tackling these inherent difficulties (Vuister et al., 1994). In this paper we introduce the 3D ^{1}H-TOCSY-relayed ct-[^{13}C,^{1}H]-HMQC experiment, which promises to be a valuable addition to the arsenal of approaches available for identification of aromatic spin systems in ^{13}C-labeled proteins.

Methods

The 3D ^{1}H-TOCSY-relayed ct-[^{13}C,^{1}H]-HMQC experiment correlates the chemical shift of a given aromatic proton with that of the attached carbon and, provided

*Present address: Departement für Pharmazie, ETH, CH-8057 Zürich, Switzerland.
**To whom correspondence should be addressed.

that the total correlation mixing time is chosen to be sufficiently short to prevent multiple ^1H relays, with those of one or two vicinal protons (Fig. 1). The design of the new experiment (Fig. 2A) is based on the following considerations: ^{13}C frequency labeling is performed in a ct fashion (Vuister and Bax, 1992) to eliminate the large one-bond scalar couplings between aromatic carbons (~60 Hz; Krivdin and Kalabin, 1989), which ensures sufficient resolution along the ^{13}C frequency axis (compare Figs. 3A and B). The ct delay is also used for the generation of ^1H-^1H antiphase magnetization, for which the transfer into in-phase magnetization of the neighbouring proton by the subsequent ^1H-TOCSY relay exhibits sine characteristics, while (1 – cos) characteristics result from ^1H in-phase magnetization (Braunschweiler and Ernst, 1983). Hence, the generation of ^1H-^1H antiphase magnetization greatly enhances the magnetization relay *at short mixing times*. ^1H-^{13}C heteronuclear multiple-quantum coherence (HMQC; Müller, 1979; Bax et al., 1983) is used to overlay the ^1H and ^{13}C chemical shift evolution periods (Kay et al., 1992; Szyperski et al., 1993). Since ^1H-^{13}C zero-quantum and double-quantum coherences are to first order insensitive to heteronuclear dipolar relaxation (Griffey and Redfield, 1987; Bax et al., 1990), the use of multiple-quantum coherence also results in increased sensitivity, in particular for large proteins with long overall rotational correlation times. Since the ct-HMQC scheme can be implemented with application of as few as five radiofrequency (rf) pulses before the ^1H-TOCSY mixing (Fig. 2A), magnetization losses due to B_1 inhomogeneity of the rf pulses are small.

The transfer amplitude of the 3D ^1H-TOCSY-relayed ct-[^{13}C,^1H]-HMQC experiment (Fig. 2A) was evaluated using the product operator formalism (Sørensen et al., 1983), where the ^1H-TOCSY relay was treated using spin

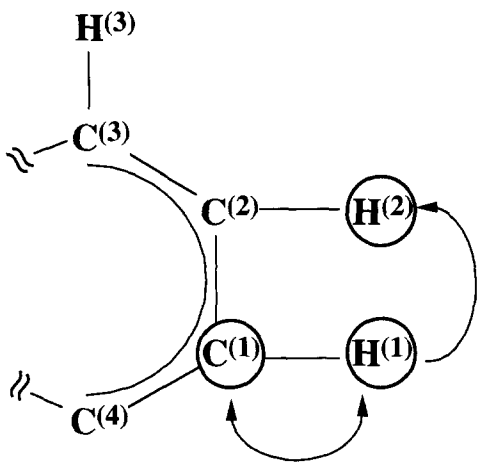

Fig. 1. Magnetization transfer pathway of the 3D ^1H-TOCSY-relayed ct-[^{13}C,^1H]-HMQC experiment. The HMQC and the ^1H-TOCSY magnetization transfers are represented by a double- and a single-headed arrow, respectively.

modes (Braunschweiler and Ernst, 1983) in a two-proton approximation. Thereby, we retained only terms resulting in observable magnetization during the detection period and only those trigonometric functions that describe the chemical shift evolution and the magnetization transfer. I and K denote the spin operators of the correlated protons $H^{(1)}$ and $H^{(2)}$, and S represents the carbon atom attached to $H^{(1)}$ ($C^{(1)}$ in Fig. 1). For heteronuclear couplings the number of intervening bonds is indicated ($^1J_{CH}$, $^3J_{CH}$), whereas J_{HH} stands for $^3J_{HH}$ throughout. The transverse proton magnetization present after the first 90° pulse on protons (a in Fig. 2A) is given by:

$$\sigma^M(a) = -I_y \qquad (1)$$

where the superscript M denotes the HMQC-type experiment. During the delay τ the scalar coupling $^1J(^{13}C,^1H)$ evolves, so that the first 90° (^{13}C) pulse generates two-spin coherence. With $\tau = 1/2\ ^1J(^{13}C,^1H)$, at time b (Fig. 2A) we thus have:

$$\sigma^M(b) = -2I_xS_y \qquad (2)$$

This term evolves during t_1 and t_2 with the chemical shifts of $C^{(1)}$ and $H^{(1)}$, ω_S and ω_I, respectively (Fig. 1). Furthermore, depending on the position of the aromatic proton, the transverse ^1H magnetization dephases due to the influence of $^3J(^{13}C,^1H)$ heteronuclear spin–spin couplings, which are between 4.5 and 8.5 Hz for aromatic compounds such as naphthalene or biphenyl (Hansen, 1981). Other long-range heteronuclear couplings as well as long-range homonuclear carbon–carbon couplings are much smaller (Hansen, 1981; Horak et al., 1985) and in the following their effects are therefore neglected. Then, m three-bond ^1H-^{13}C scalar couplings must be considered during $T + 2\tau - t_1 - t_2$ (in Fig. 1, $^3J(^{13}C^{(3)},^1H^{(1)})$ is one of the couplings considered here; generally, $2 \le m \le 3$ in the four common aromatic amino acids). Likewise, transverse ^{13}C magnetization dephases due to n three-bond ^1H-^{13}C couplings during $T - t_1 - t_2$ (e.g., $^3J(^{13}C^{(1)},^1H^{(3)})$ in Fig. 1; generally, $1 \le n \le 4$ in the four common aromatic amino acids). In contrast, provided that $T = 1/^1J(^{13}C,^{13}C)$ and assuming weak scalar coupling, dephasing due to $^1J(^{13}C,^{13}C)$ is refocussed and can be accounted for by introduction of a factor $(-1)^k$ (k denotes the number of attached carbons; Vuister and Bax, 1992). The second 90°(^{13}C) pulse recreates single-quantum antiphase coherence, which refocuses during τ. Considering the evolution of the density matrix due to J_{HH}, the magnetization present before the TOCSY mixing scheme (c in Fig. 2A) is then given by:

$$\begin{aligned}\sigma^M(c) = (-1)^k \cos^m[\pi\ ^3J_{CH}\ (T + 2\tau - t_1 - t_2)] \\ \cos^n[\pi\ ^3J_{CH}\ (T - t_1 - t_2)]\ \cos(\omega_S t_1)\ \cos(\omega_I t_2) \qquad (3) \\ \times \{ -I_y \cos[\pi\ J_{HH}\ (T + 2\tau)] + 2I_xK_z \sin[\pi\ J_{HH}\ (T + 2\tau)] \}\end{aligned}$$

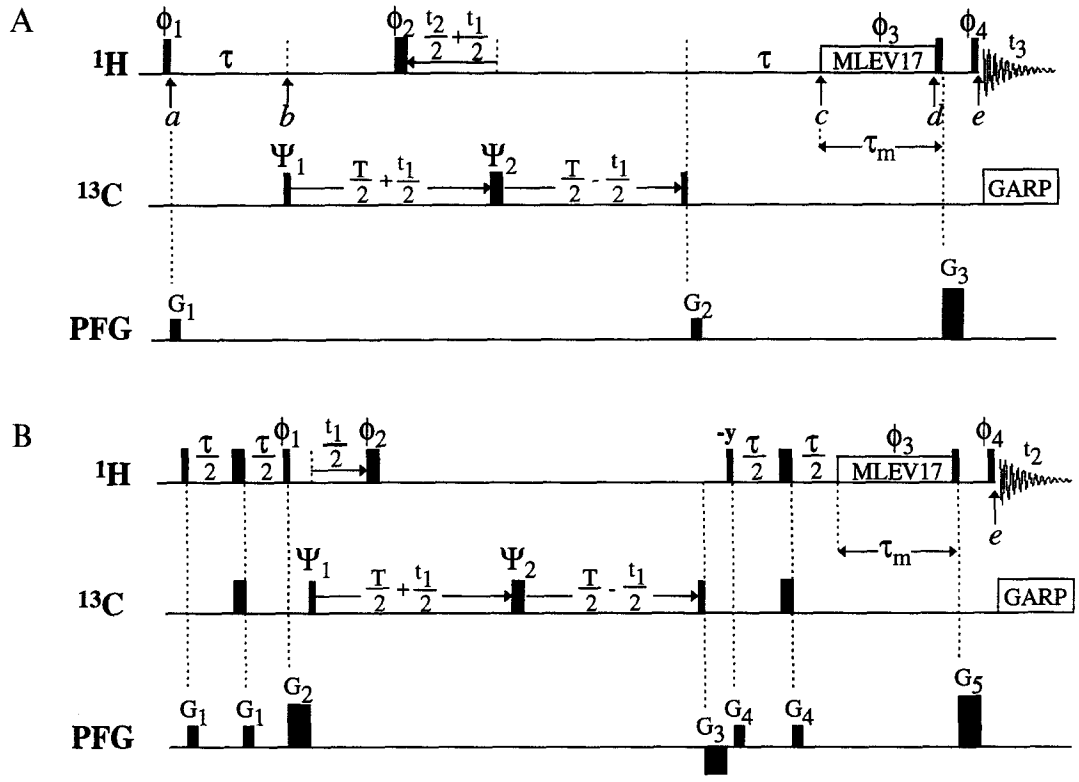

Fig. 2. Experimental schemes for (A) 3D ^{1}H-TOCSY-relayed ct-[^{13}C,^{1}H]-HMQC and (B) 2D ^{1}H-TOCSY-relayed ct-[^{13}C,^{1}H]-HSQC, with indication of the parameters used for the presently reported experiments. 90° and 180° ^{1}H and ^{13}C pulses are indicated by thin and thick vertical bars, respectively, and phases are indicated above the pulses. When no phase is marked, the pulse was applied along the x-axis. Prior to the first proton pulse, the proton carrier was placed near the center of the aromatic region at 6.9 ppm, and it was then switched to the position of the water line (4.76 ppm at 26 °C) during the z-filter delay. The carbon carrier was set to 126 ppm. Pulsed field gradients were used for coherence pathway rejection and suppression of the water signal (Bax and Pochapsky, 1992; Wider and Wüthrich, 1993). All gradients are block-shaped and have amplitudes of 5 G/cm and durations of 0.5 ms, except for those applied to select for longitudinal proton magnetization (20 G/cm and 1 ms for G_3 in A and for G_5 in B; 15 G/cm and 1 ms, and −8 G/cm and 1 ms for G_2 and G_3, respectively, in B). A recovery delay of 200 μs was introduced between gradients and immediately following rf pulses. The constant-time period T was adjusted to $1/^1J(^{13}C,^{13}C) = 16.6$ ms, and τ was set to 3.0 ms. For proton isotropic mixing, a clean-TOCSY (Griesinger et al., 1988) pulse train using the MLEV17 supercycle (Levitt et al., 1982) was applied during $\tau_m = 20$ ms. Carbon decoupling during acquisition was accomplished with a GARP decoupling scheme (Shaka et al., 1985) using a 2.5 kHz rf field. The 90° pulse lengths were 12 μs for ^{1}H and 20 μs for ^{13}C. Phase cycling: (A) $\psi_1 = 8(x,-x)$; $\psi_2 = 4(x),4(y),4(-x),4(-y)$; $\phi_1 = 16(x)$; $\phi_2 = 2(2(x),2(y),2(-x),2(-y))$; $\phi_3 = 2(4(x),4(-x))$; $\phi_4 = 4(2(x),2(-x))$; rec. $= 2(2(x,-x),2(-x,x))$; (B) $\psi_1 = 8(x,-x)$; $\psi_2 = 2(2(x),2(y),2(-x),2(-y))$; $\phi_1 = 2(4(y),4(-y))$; $\phi_2 = 2(4(x),4(-x))$; $\phi_3 = 8(x),8(-x)$; $\phi_4 = 4(2(x),2(-x))$; rec. $= 2(2(x,-x),2(-x,x))$. Quadrature detection in t_1 and t_2 was achieved by altering the phases ϕ_1 and ψ_1 according to the States-TPPI method (Marion et al., 1989).

For the following description of the subsequent ^{1}H isotropic mixing in a two-spin approximation, $\sigma^M(c)$ is abbreviated as:

$$\sigma^M(c) = -\alpha I_y + 2\beta I_x K_z \quad (4)$$

where the definitions of α and β are evident from Eq. 3. $\sigma^M(c)$ is then transformed into the basis set formed by spin modes (Braunschweiler and Ernst, 1983), which are defined as:

$$\Sigma_y = 1/2\,(I_y + K_y) \quad (5a)$$

$$\Sigma_{zx} = (I_z K_x + I_x K_z) \quad (5b)$$

$$\Delta_y = 1/2\,(I_y - K_y) \quad (5c)$$

$$\Delta_{zx} = (I_z K_x - I_x K_z) \quad (5d)$$

yielding:

$$\sigma^M(c) = -\alpha(\Sigma_y + \Delta_y) + \beta(\Sigma_{zx} - \Delta_{zx}) \quad (6)$$

The density matrix describing the magnetization after the isotropic mixing period, τ_m, is then given by:

$$\sigma^M(d) = -\alpha\Sigma_y + \beta\Sigma_{zx} - \Delta_{zx}\,[\beta\cos(2\pi J_{HH}\tau_m) + \alpha\sin(2\pi J_{HH}\tau_m)] - \Delta_y\,[\alpha\cos(2\pi J_{HH}\tau_m) - \beta\sin(2\pi J_{HH}\tau_m)] \quad (7)$$

Considering that the subsequent z-filter (Sørensen et al., 1984) destroys dispersive ^{1}H-^{1}H antiphase magnetization aligned along the x-axis, and neglecting zero-quantum terms that are not destroyed by the z-filter (Rance et al., 1985; Subramanian and Bax, 1987), the back-transform-

ation of $\sigma^M(d)$ into Cartesian operators yields, with inclusion of the trigonometric terms of Eq. 3, the density matrix describing the observable magnetization at the beginning of the detection period (e in Fig. 2A):

$$\sigma^M(e) = (-1)^k \cos^m[\pi\, {}^3J_{CH}\,(T + 2\tau - t_1 - t_2)]$$
$$\cos^n[\pi\, {}^3J_{CH}\,(T - t_1 - t_2)]\cos(\omega_S t_1)\cos(\omega_I t_2)$$
$$\times \{-I_y/2\ \{\cos[\pi\, J_{HH}\,(T + 2\tau)]$$
$$+ \cos[\pi\, J_{HH}\,(T + 2\tau)]\cos[2\pi\, J_{HH}\,\tau_m] \quad (8a)$$
$$- \sin[\pi\, J_{HH}\,(T + 2\tau)]\sin[2\pi\, J_{HH}\,\tau_m]\}$$
$$-K_y/2\ \{\cos[\pi\, J_{HH}\,(T + 2\tau)]$$
$$- \cos[\pi\, J_{HH}\,(T + 2\tau)]\cos[2\pi\, J_{HH}\,\tau_m] \quad (8b)$$
$$+ \sin[\pi\, J_{HH}\,(T + 2\tau]\sin[2\pi\, J_{HH}\,\tau_m]\}\}$$

The terms 8a and 8b represent the direct and relay peaks, respectively, which are observed in a 3D ^{1}H-TOCSY-relayed ct-[^{13}C,^{1}H]-HMQC experiment.

In order to compare the HMQC experiment with its HSQC counterpart, we implemented a 2D ^{1}H-TOCSY-relayed ct-[^{13}C,^{1}H]-HSQC experiment (Fig. 2B). A treatment analogous to that described in Eqs. 1–7 leads to the density matrix:

$$\sigma^S(e) = (-1)^k \cos^{2m}[\pi\, {}^3J_{CH}\,\tau]\cos(\omega_S t_1)$$
$$\times \{-I_y/2\ \{\cos[\pi\, J_{HH}\,\tau]$$
$$+ \cos[\pi\, J_{HH}\,\tau]\cos[2\pi\, J_{HH}\,\tau_m] \quad (9a)$$
$$- \sin[\pi\, J_{HH}\,\tau]\sin[2\pi\, J_{HH}\,\tau_m]\}$$
$$-K_y/2\ \{\cos[\pi\, J_{HH}\,\tau]$$
$$- \cos[\pi\, J_{HH}\,\tau]\cos[2\pi\, J_{HH}\,\tau_m] \quad (9b)$$
$$+ \sin[\pi\, J_{HH}\,\tau]\sin[2\pi\, J_{HH}\,\tau_m]\}\}$$

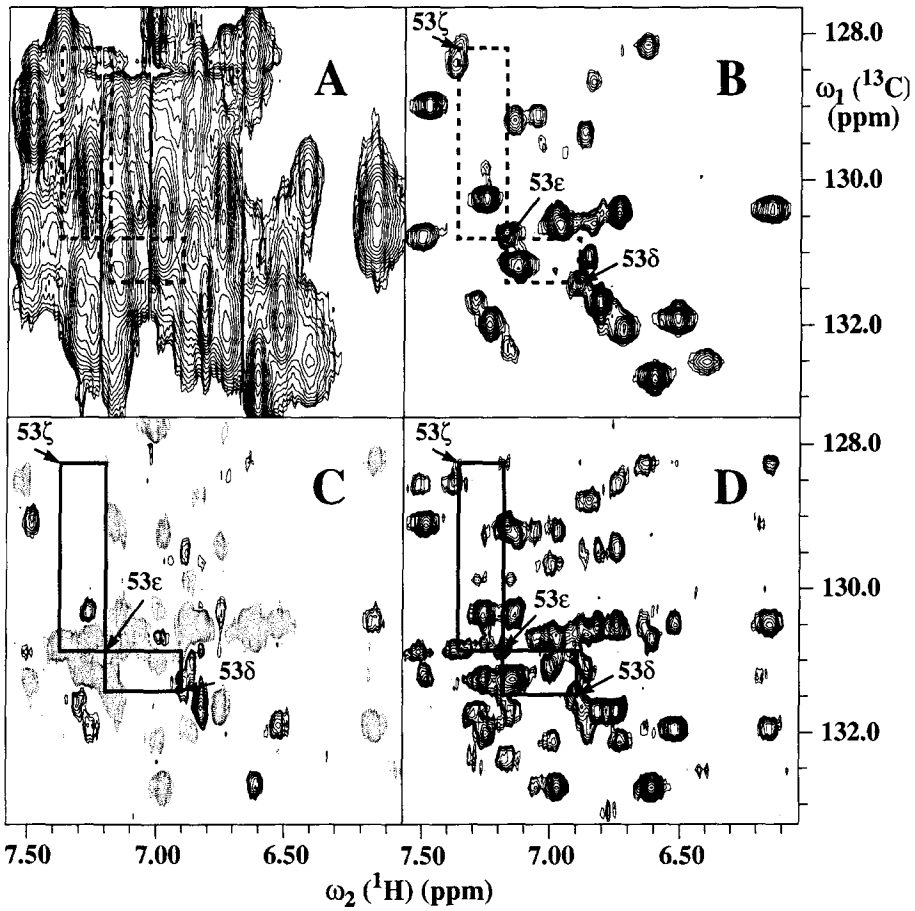

Fig. 3. Contour plots of four different 2D ^{1}H-^{13}C correlation experiments performed with cyclophilin A, which display a spectral region containing resonances of phenylalanyl residues. (A) 2D [^{13}C,^{1}H]-HSQC (Bodenhausen and Ruben, 1980). (B) 2D ct-[^{13}C,^{1}H]-HSQC (Vuister and Bax, 1992). (C) 2D ct-HCCH-COSY (Ikura et al., 1991). (D) 2D ^{1}H-TOCSY-relayed ct-[^{13}C,^{1}H]-HMQC recorded with $\tau_m = 20$ ms (Fig. 2A). All spectra were recorded with a 1.5 mM solution of uniformly ^{13}C-labeled cyclophilin A in D_2O (pD = 6.5, T = 26 °C) on a Bruker AMX-600 spectrometer as data matrices of 1024 (t_2) * 78 (t_1) (A, B, D) or 1024 (t_2) * 65 (t_1) (C) complex data points, with $t_{1,max}$ (^{13}C) = 16 ms (A, B, D) or 12.5 ms (C), and $t_{2,max}$ (^{1}H) = 150 ms. A total of 128 scans were acquired, resulting in measurement times of 9 h each for A, B and D, and 6.8 h for C. Time-domain data were extended by linear prediction along t_1, and digital filtering was performed with cosine window functions in both dimensions (DeMarco and Wüthrich, 1976). The digital resolution after zero-filling was 9.5 Hz along ω_1(^{13}C) and 1.7 Hz along ω_2(^{1}H). The spectra were processed with the program PROSA (Güntert et al., 1992). In C and D the pattern of cross peaks that correlate the three direct ^{13}C-^{1}H cross peaks of Phe^{53} (identified as 53δ, 53ε and 53ζ) is indicated with solid lines; in A and B the same pattern has been drawn with broken lines to indicate that no connectivities are expected in these experiments.

TABLE 1
COMPARISON OF RELATIVE PEAK INTENSITIES FOR WELL-RESOLVED RESONANCES OF TRYPTOPHAN AND PHENYLALANINE IN CYCLOPHILIN A

	2D ^{1}H-TOCSY-relayed ct-HMQC[a]	2D ^{1}H-TOCSY-relayed ct-HSQC	2D ct-HCCH-TOCSY[b]	2D ct-HCCH-COSY[c]
Tryptophan				
relay peaks	1.00	0.49	0.42	1.09
direct peaks	1.00	0.98	0.14	0.51
sum[d]	2.00	1.47	0.56	1.60
Phenylalanine				
relay peaks	1.00	0.66	0.89	1.29
direct peaks	1.00	1.18	0.48	0.44
sum[d]	2.00	1.84	1.37	1.73

[a] The intensities observed were measured in 2D spectra recorded with the experimental schemes of Fig. 2.
[b] ^{13}C isotropic mixing was achieved by applying a 3 ms DIPSI-2 (Shaka et al., 1988) sequence using an rf power of 7 kHz.
[c] The constant-time delay in the 2D ct-HCCH-COSY experiment (Ikura et al., 1991) was tuned to $3/(4\,{}^1J_{CC})$ to yield carbon–carbon antiphase coherence for the COSY transfer, and the delay for refocusing of this coupling was set to $1/(4\,{}^1J_{CC})$, so that the ^{13}C magnetization remained transverse for the same duration as in the ^{1}H-TOCSY-relayed experiments. Measured peak intensities were multiplied by a factor of 4/3 in order to compensate for the shorter measuring time used for this experiment (see legend to Fig. 3).
[d] The last row contains the summed intensities, which are a measure of the total magnetization retained in the experiment.

where the superscript S denotes the HSQC-type experiment.

Results and Discussion

We used the presently introduced HMQC experiment (Fig. 2A) for resonance assignments of uniformly ^{13}C-labeled cyclophilin A, a protein with 165 amino acid residues and a molecular weight of about 18 kDa, which contains 22 aromatic residues (15 phenylalanines, 4 histidines, 2 tyrosines and 1 tryptophan). We also compared the relative sensitivity of the experiment of Fig. 2A with other experiments in use for aromatic spin system identification.

In Table 1 the intensities of well-resolved direct and relayed peaks observed in a 2D ^{1}H-TOCSY-relayed ct-[^{13}C,^{1}H]-HMQC spectrum recorded with $\tau_m = 20$ ms (Fig. 3D) are compared with those obtained from 2D ^{1}H-TOCSY-relayed ct-[^{13}C,^{1}H]-HSQC ($\tau_m = 20$ ms), 2D ct-HCCH-TOCSY ($\tau_m = 3$ ms; Damberger et al., 1994), and 2D ct-HCCH-COSY (Ikura et al., 1991). Two-dimensional ^{1}H-TOCSY-relayed ct-[^{13}C,^{1}H]-HMQC has more intense relay peaks and higher overall peak intensity than either 2D ^{1}H-TOCSY-relayed ct-[^{13}C,^{1}H]-HSQC or 2D ct-HCCH-TOCSY. For the latter experiment, the reduced signal intensity is primarily due to the fact that quaternary carbon atoms act as coherence sinks during ^{13}C-TOCSY mixing, since the transverse magnetization transferred to quaternary carbons is not converted back into observable proton magnetization. Similarly, the overall sensitivity ('sum' in Table 1) of 2D ct-HCCH-COSY is reduced, and here the spectral analysis is further hampered by the fact that direct peaks and relay peaks have opposite sign and may be mutually cancelled in crowded spectral regions (Fig. 3C).

The overlap of direct and relay peaks seen in the 2D ^{1}H-TOCSY-relayed ct-[^{13}C,^{1}H]-HMQC experiment (Fig. 3D) is neatly resolved in the corresponding 3D experiment (Fig. 4A). With the presently used short mixing time of 20 ms, multiple relays are generally not observed for proteins, so that the experiment essentially provides ^{1}H-^{1}H COSY information. This is a suitable basis for identification of the aromatic spin systems, since the different carbon positions exhibit characteristically different and only slightly conformation-dependent ^{13}C chemical shifts (Wüthrich, 1976). Furthermore, with this set-up of ^{1}H-TOCSY-relayed ct-[^{13}C,^{1}H]-HMQC, usually only the ε carbon of phenylalanine, and the ζ3 and η2 carbons of tryptophan give rise to two relay peaks (Fig. 4A; if the two ε-proton chemical shifts of phenylalanine are not degenerate, the ζ proton will also give rise to two relay peaks). Whenever multiple relays are desirable, 2D ct-HCCH-TOCSY complements the ^{1}H-TOCSY-relayed ct-[^{13}C,^{1}H]-HMQC experiment. With a mixing time of about 7–10 ms for 2D ct-HCCH-TOCSY, the $^{13}C^{\delta 1}$-$^1H^{\delta 1}$ resonance of tryptophan can be correlated with the protons of the six-membered ring of the indole moiety (Fig. 4B). This greatly facilitates the sequence-specific assignment of tryptophan, since the δ1 proton can readily be linked to the $^{13}C^{\alpha}H$-$^{13}C^{\beta}H_2$ fragment of the same residue, either via NOEs (Wüthrich, 1986) or via scalar connectivities (Yamazaki et al., 1993). With this combined use of 3D ^{1}H-TOCSY-relayed ct-[^{13}C,^{1}H]-HMQC and 2D ct-HCCH-TOCSY, nearly complete assignments of the aromatic spin systems of cyclophilin A were obtained, as will be described elsewhere (M. Ottiger, O. Zerbe and K. Wüthrich, to be published).

The encouraging results obtained in practice with ^{1}H-TOCSY-relayed ct-[^{13}C,^{1}H]-HMQC (Figs. 3D and 4) are largely based on favorable sensitivity relative to other experiments in use for aromatic spin system identification.

To establish this aspect in a more quantitative fashion, we compared the buildup rates of relayed in-phase magnetization for the HMQC and HSQC experiments in 2D spectra with ^{13}C-labeled tyrosine, using the experimental schemes of Fig. 2A (with $t_2(^1H) = 0$) and Fig. 2B, respectively (Fig. 5). Inspection of Eqs. 8 and 9 reveals two important differences between the HMQC and HSQC experiments. First, the influence of passive $^3J(^{13}C,^1H)$ couplings is negligible for the 2D HSQC experiment, since $\cos[\pi\ ^3J_{CH}\ \tau] \approx 1$. In contrast, the signal of the HMQC experiment is reduced by:

$$A = 1 - (1/T^2) \int_0^T \int_0^T \cos^{m}[\pi\ ^3J_{CH}\ (T + 2\tau - t_1 - t_2)] \cos^{n}[\pi\ ^3J_{CH}\ (T - t_1 - t_2)]\, dt_1\, dt_2 \quad (10)$$

where m and n are defined as in Eq. 3. Considering that $^3J_{CH}$ scalar couplings are between 4.5 and 8.5 Hz (Hansen, 1981), we estimated A values for all aromatic positions using $^3J_{CH} = 7$ Hz in Eq. 10. The signal attenuation was thus found to vary between 12 and 19% for the 2D HMQC experiment with $t_2 = 0$ and omitting the integra-

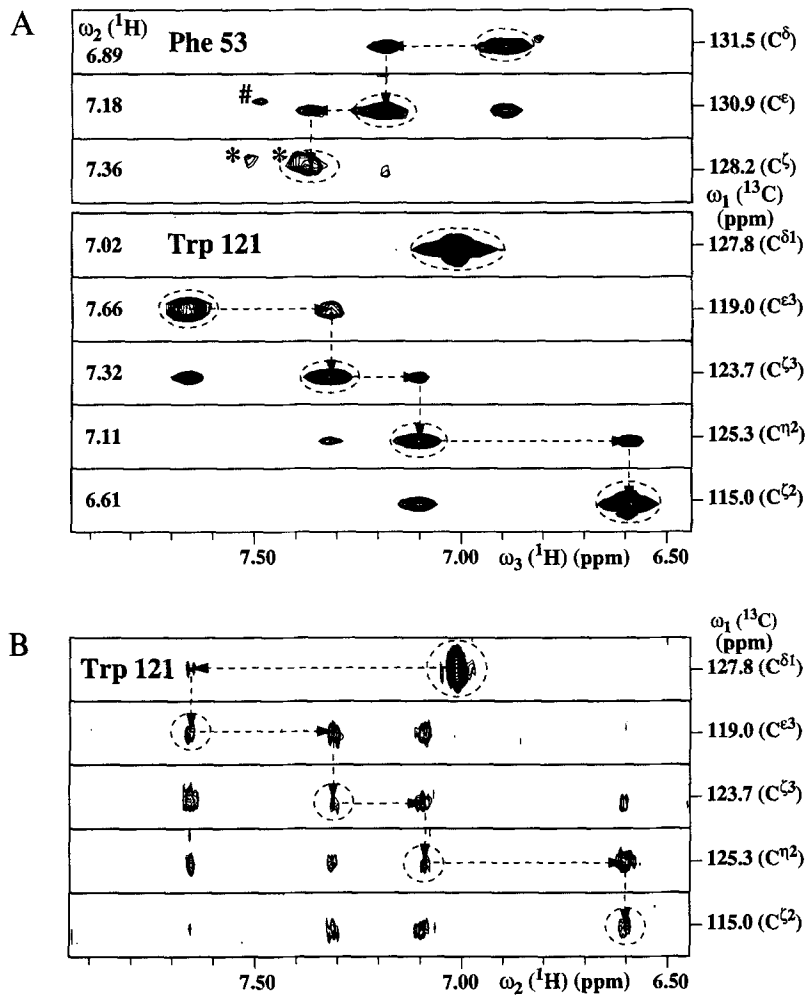

Fig. 4. (A) Contour plots of $[\omega_1(^{13}C), \omega_3(^1H)]$ strips from a 3D ^{1}H-TOCSY-relayed ct-HMQC experiment recorded with a 1.5 mM solution of cyclophilin A (the same sample as in Fig. 3) on a Bruker AMX-600 spectrometer using the experimental scheme of Fig. 2A with a TOCSY mixing time of $\tau_m = 20$ ms. 1024 (t_3) * 32 (t_2) * 78 (t_1) complex points were accumulated, yielding $t_{1,max}$ (^{13}C) = $t_{2,max}$ (^{1}H) = 16 ms and $t_{3,max}$ (^{1}H) = 150 ms. Sixteen scans per increment were acquired, resulting in a measuring time of about 36 h. Prior to Fourier transformation, the data matrix was extended by linear prediction along t_1 and t_2, and digital filtering was performed with cosine window functions in all dimensions (DeMarco and Wüthrich, 1976). The digital resolution after zero-filling was 15.3 Hz along $\omega_1(^{13}C)$, 18.9 Hz along $\omega_2(^1H)$ and 6.7 Hz along $\omega_3(^1H)$. The spectrum was processed using the program PROSA (Güntert et al., 1992). The strips were taken at the aromatic ^{1}H chemical shifts of Phe^{53} and Trp^{121} along ω_2, and are centered about the corresponding ^{13}C shifts in ω_1. Additional peaks in the strips of Phe^{53} belong to Phe^{8} (#) and Phe^{83} (*). (B) Contour plots of $[\omega_1(^{13}C), \omega_2(^1H)]$ strips of Trp^{121}, taken from a 2D ct-HCCH-TOCSY spectrum recorded with an isotropic mixing period of 7.5 ms and employing a 7 kHz DIPSI-3 sequence (Shaka et al., 1988). The spectrum was recorded with the same sample as in (A), as a data matrix of 2048 (t_2) * 115 (t_1) complex points on a Varian UnityPlus 750 MHz spectrometer, yielding $t_{1,max}$ (^{13}C) = 16 ms and $t_{2,max}$ (^{1}H) = 205 ms. Per increment 128 scans were acquired, resulting in a measuring time of about 13 h. The spectrum was processed identically to those in Fig. 3. The digital resolution after zero-filling was 14 Hz along $\omega_1(^{13}C)$ and 2.4 Hz along $\omega_2(^1H)$. In (A) and (B) the direct ^{13}C-^{1}H cross peaks are circled with a broken line, and assignment pathways for the aromatic spin systems are indicated with arrows.

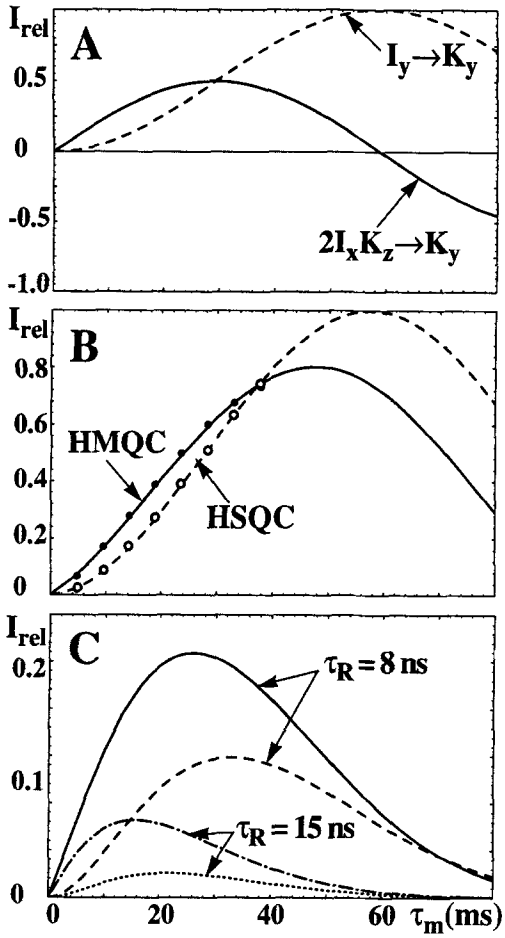

Fig. 5. ^{1}H-TOCSY magnetization transfer profiles presented as plots of the relative transfer rate, I_{rel}, versus the mixing time τ_m. (A) Antiphase (I_xK_z) to in-phase (K_y) (solid line) and in-phase (I_y) to in-phase (K_y) (dashed line) transfer calculated with $J_{HH} = 8.5$ Hz. (B) The curves represent the results of similar calculations as in (A) for the linear combinations of in-phase and antiphase magnetization present in 2D ^{1}H-TOCSY-relayed ct-[^{13}C,^{1}H]-HMQC (solid line) and 2D ^{1}H-TOCSY-relayed ct-[^{13}C,^{1}H]-HSQC (dotted line) experiments at the start of the isotropic mixing period (Eqs. 8b and 9b, respectively). For the HMQC experiment, the attenuation factor A was estimated with Eq. 10 to be 0.12 (see text). The relative intensities of the relay peaks observed for ^{13}C-labeled tyrosine in 2D ^{1}H-TOCSY-relayed ct-[^{13}C,^{1}H]-HMQC and 2D ^{1}H-TOCSY-relayed ct-[^{13}C,^{1}H]-HSQC experiments recorded with varying mixing time are presented as filled and open circles, respectively. (C) The same calculation as in (B), except that transverse relaxation was also considered, as described in the text. The interatomic distances were set to $r_{HH} = 2.51$ Å and $r_{CH} = 1.09$ Å, and a field strength of 14.1 T was used for the calculations. The solid and dashed lines were calculated for 2D ^{1}H-TOCSY-relayed ct-[^{13}C,^{1}H]-HMQC and 2D ^{1}H-TOCSY-relayed ct-[^{13}C,^{1}H]-HSQC, respectively, assuming a correlation time of $\tau_R = 8$ ns for the overall rotational tumbling. The dashed–dotted and dotted lines were likewise calculated for the HMQC and HSQC experiments, respectively, using $\tau_R = 15$ ns.

tion over t_2, and between 5 and 8% for the 3D HMQC experiment (Fig. 2A). Second, we have that $\sin[\pi J_{HH}(T + 2\tau)] \gg \sin[\pi J_{HH}\tau]$ for $J_{HH} = 8.5$ Hz, $T = 1/{}^1J(^{13}C,^{13}C)$ and $\tau \leq 1/2\,{}^1J(^{13}C,^1H)$. As a result, at short mixing times the ^{1}H magnetization transfer is more efficient in the HMQC experiment. This is due to the fact that at time c (Fig. 2) the HMQC experiment contains a significantly larger fraction of ^{1}H-^{1}H antiphase magnetization, which at short mixing times up to about 27 ms results in increased buildup of relayed in-phase magnetization (Fig. 5A). Figure 5B compares the predicted τ_m dependence of the relative relay-peak intensities of the HMQC and HSQC experiments with the buildup of the cross-peak intensities measured for ^{13}C-labeled tyrosine. The measured relative relay-peak intensities closely follow the curves predicted by Eqs. 8b and 9b. For $\tau_m \approx 20$ ms, the intensity of the relay peak in the HMQC experiment with tyrosine is increased by about 30%, and a comparable gain in sensitivity at short mixing times can be anticipated for the ^{1}H spin systems of phenylalanine and tryptophan. Overall, we thus have that the signal attenuation from passive $^3J_{CH}$ couplings is significantly smaller than the gain originating from the accelerated ^{1}H magnetization transfer due to the generation of ^{1}H-^{1}H antiphase magnetization during the constant-time delay in HMQC.

Transverse relaxation during the constant-time period is a major source of sensitivity losses in ^{1}H-TOCSY-relayed ct-[^{13}C,^{1}H] correlation spectroscopy. While transverse ^{13}C relaxation in HSQC experiments is dominated by heteronuclear dipolar coupling with the attached proton, relaxation of ^{1}H-^{13}C zero-quantum and double-quantum coherences in HMQC experiments is to first order insensitive to dipolar heteronuclear coupling (Bax et al., 1990). Hence, relaxation of these coherences is dominated by ^{1}H-^{1}H dipolar couplings and is thus comparable to relaxation of single-quantum coherences of protons attached to ^{12}C. We calculated the influence of transverse relaxation on the time course of the signal intensities in 2D ^{1}H-TOCSY-relayed HSQC and ^{1}H-TOCSY-relayed HMQC experiments (Fig. 5C) using Eqs. 2a–c in the paper by Bax et al. (1990), with the following assumptions: (i) relaxation of ^{1}H single-quantum coherences and ^{1}H magnetization of aromatic protons present during the isotropic mixing period τ_m and the delays τ (Fig. 2) is entirely due to heteronuclear dipolar coupling with the attached ^{13}C and to ^{1}H-^{1}H dipolar coupling with two vicinal aromatic protons; (ii) ^{13}C single-quantum coherence relaxation is entirely due to dipolar coupling with the attached proton; (iii) relaxation of ^{1}H-^{13}C zero-quantum and double-quantum coherences is entirely due to ^{1}H-^{1}H dipolar coupling with two vicinal aromatic protons. The results obtained clearly support the previously advanced notion (Bax et al., 1990; Seip et al., 1992; Grzesiek and Bax, 1995b; Grzesiek et al., 1995) that [^{13}C,^{1}H]-HMQC-type experiments may become superior to their HSQC counterparts when the overall rotational correlation time, τ_R, approaches the slow tumbling limit. Figure 5C shows that for large proteins ($\tau_R = 15$ ns) a 2D ^{1}H-TOCSY-relayed ct-[^{13}C,^{1}H]-HMQC experiment, performed with a mixing time of about 20 ms can be expected to be roughly two- to threefold more sensitive than its HSQC analogue.

For 3D versions of ^{1}H-TOCSY-relayed ct-[^{13}C,^{1}H] correlation spectroscopy, the use of HMQC is mandatory in order to obtain workable sensitivity for larger proteins. Intrinsically, when compared with 2D NMR, the sensitivity of 3D experiments is reduced by a factor $\sqrt{2}$ due to phase-sensitive detection in the second indirect dimension (Bax and Grzesiek, 1993). In addition, the ^{1}H chemical shift evolution in the indirect dimension t_2 in a (hypothetical) 3D HSQC experiment would not be overlaid with the ^{13}C chemical shift evolution in t_1, so that the additional delay for t_2 would lead to significant additional losses arising from transverse ^{1}H relaxation.

Conclusions

The presently introduced 3D ^{1}H-TOCSY-relayed ct-[^{13}C,^{1}H]-HMQC experiment for assignment of aromatic spin systems in uniformly ^{13}C-labeled proteins exploits transfer of antiphase to in-phase magnetization to accelerate ^{1}H total correlation at short mixing times. Due to its high inherent sensitivity, the experiment has the potential for complete identification of the aromatic spin systems in larger proteins. The interest in complete assignments of the aromatic proton spin systems in proteins is clearly documented by the following: for the protein used here for illustration purposes, cyclophilin A, a recent high-quality NMR solution structure determination (M. Ottiger, O. Zerbe and K. Wüthrich, to be published) was based on 4097 NOE upper distance constraints, 501 of which involve aromatic protons. The mean pairwise global root-mean-square deviation (rmsd) relative to the mean coordinates calculated for all heavy atoms of residues 2 to 165 increased from 0.86 to 1.11 Å when the NOEs involving aromatic protons were omitted from the structure calculation. This increase is significant, but due to the compact β-barrel folding topology of cyclophilin A (Spitzfaden et al., 1994), it is smaller than for certain other proteins where the spatial arrangement of the secondary structure elements does not per se impose tight packing constraints. For example, for the 15 kDa plant defense protein P14A (T. Szyperski, C. Fernández, T. Bruyère, E. Mösinger and K. Wüthrich, to be published) an input of 1712 NOE upper distance constraints was used, 303 of which involved aromatic protons. P14A has a complex α/β folding topology, and the rmsd values relative to the mean coordinates calculated for all heavy atoms with and without inclusion of NOEs involving aromatic protons are 1.29 and 2.24 Å, respectively.

References

Archer, S.J., Vinson, V.K., Pollard, T.D. and Torchia, D.A. (1993) *Biochemistry*, **32**, 6680–6687.

Bax, A., Griffey, R.H. and Hawkins, B.L. (1983) *J. Magn. Reson.*, **55**, 301–315.

Bax, A., Ikura, M., Torchia, D.A., Kay, L.E. and Tschudin, R. (1990) *J. Magn. Reson.*, **86**, 304–318.

Bax, A. and Pochapsky, S.S. (1992) *J. Magn. Reson.*, **99**, 638–643.

Bax, A. and Grzesiek, S. (1993) *Acc. Chem. Res.*, **26**, 131–138.

Bodenhausen, G. and Ruben, D.J. (1980) *Chem. Phys. Lett.*, **69**, 185–189.

Braunschweiler, L. and Ernst, R.R. (1983) *J. Magn. Reson.*, **53**, 521–528.

Damberger, F.F., Pelton, J.G., Harrison, C.J., Nelson, H.C.M. and Wemmer, D.E. (1994) *Protein Sci.*, **3**, 1806–1821.

DeMarco, A. and Wüthrich, K. (1976) *J. Magn. Reson.*, **24**, 201–204.

Griesinger, C., Otting, G., Wüthrich, K. and Ernst, R.R. (1988) *J. Am. Chem. Soc.*, **110**, 7870–7872.

Griffey, R.H. and Redfield, A.G. (1987) *Q. Rev. Biophys.*, **19**, 51–82.

Grzesiek, S. and Bax, A. (1995a) *J. Am. Chem. Soc.*, **117**, 6527–6531.

Grzesiek, S. and Bax, A. (1995b) *J. Biomol. NMR*, **6**, 335–339.

Grzesiek, S., Kuboniwa, H., Hinck, A.P. and Bax, A. (1995) *J. Am. Chem. Soc.*, **117**, 5312–5315.

Güntert, P., Dötsch, V., Wider, G. and Wüthrich, K. (1992) *J. Biomol. NMR*, **2**, 619–629.

Hansen, P.E. (1981) *Prog. NMR Spectrosc.*, **14**, 175–296.

Horak, R.M., Steyn, P.S. and Vleggaar, R. (1985) *Magn. Reson. Chem.*, **23**, 995–1039.

Ikura, M., Kay, L.E., Tschudin, R. and Bax, A. (1990) *J. Magn. Reson.*, **86**, 204–209.

Ikura, M., Kay, L.E. and Bax, A. (1991) *J. Biomol. NMR*, **1**, 299–304.

Kay, L.E., Wittekind, M., McCoy, M.A., Friedrichs, M.S. and Müller, L. (1992) *J. Magn. Reson.*, **98**, 443–450.

Krivdin, L.B. and Kalabin, G.A. (1989) *Prog. NMR Spectrosc.*, **21**, 293–448.

Levitt, M.H., Freeman, R. and Frenkiel, T. (1982) *J. Magn. Reson.*, **75**, 328–330.

Logan, T.M., Zhou, M.M., Nettesheim, D.G., Meadows, R.P., Van Etten, R.L. and Fesik, S.W. (1994) *Biochemistry*, **33**, 11087–11096.

Marion, D., Ikura, M., Tschudin, R. and Bax, A. (1989) *J. Magn. Reson.*, **85**, 393–399.

Müller, L. (1979) *J. Am. Chem. Soc.*, **101**, 4481–4484.

Otting, G. and Wüthrich, K. (1990) *Q. Rev. Biophys.*, **23**, 39–96.

Rance, M., Bodenhausen, G., Wagner, G., Wüthrich, K. and Ernst, R.R. (1985) *J. Magn. Reson.*, **62**, 497–510.

Seip, S., Balbach, J. and Kessler, H. (1992) *J. Magn. Reson.*, **100**, 406–410.

Shaka, A.J., Lee, C.J. and Pines, A. (1985) *J. Magn. Reson.*, **54**, 547–552.

Shaka, A.J., Lee, C.J. and Pines, A. (1988) *J. Magn. Reson.*, **77**, 274–293.

Sørensen, O.W., Eich, G.W., Levitt, M.H., Bodenhausen, G. and Ernst, R.R. (1983) *Prog. NMR Spectrosc.*, **16**, 163–192.

Sørensen, O.W., Rance, M. and Ernst, R.R. (1984) *J. Magn. Reson.*, **56**, 527–534.

Spitzfaden, C., Braun, W., Wider, G., Widmer, H. and Wüthrich, K. (1994) *J. Biomol. NMR*, **4**, 463–482.

Subramanian, S. and Bax, A. (1987) *J. Magn. Reson.*, **71**, 325–330.

Szyperski, T., Wider, G., Bushweller, J.H. and Wüthrich, K. (1993) *J. Biomol. NMR*, **3**, 127–132.

Szyperski, T., Pellecchia, M., Wall, D., Georgopoulos, C. and Wüthrich, K. (1994) *Proc. Natl. Acad. Sci. USA*, **91**, 11343–11347.

Vuister, G.W. and Bax, A. (1992) *J. Magn. Reson.*, **98**, 428–435.

Vuister, G.W., Kim, S.J., Wu, C. and Bax, A. (1994) *J. Am. Chem. Soc.*, **116**, 9206–9210.

Wider, G. and Wüthrich, K. (1993) *J. Magn. Reson. Ser. B*, **102**, 239–241.

Wüthrich, K. (1976) *NMR in Biological Research: Peptides and Proteins*, North Holland, Amsterdam.

Wüthrich, K. (1986) *NMR of Proteins and Nucleic Acids*, Wiley, New York, NY.

Yamazaki, T., Kay, J.D. and Kay, L.E. (1993) *J. Am. Chem. Soc.*, **115**, 11054–11055.